



Cite this: *New J. Chem.*, 2020, **44**, 15297

Correction: Unravelling lithiation mechanisms of iron trifluoride by *operando* X-ray absorption spectroscopy and MCR-ALS chemometric tools

F. Eveillard,^a C. Gervillie,^a C. Taviot-Guého,^a F. Leroux,^a K. Guérin,^{*a} M. T. Sougrati,^b S. Belin^c and D. Delbègue^d

DOI: 10.1039/d0nj90118k

rsc.li/njc

Correction for 'Unravelling lithiation mechanisms of iron trifluoride by *operando* X-ray absorption spectroscopy and MCR-ALS chemometric tools' by F. Eveillard et al., *New J. Chem.*, 2020, **44**, 10153–10164, DOI: 10.1039/C9NJ06321H.

The authors regret the following errors in the original manuscript.

1. The authors have provided updated Fig. 2 and Table 1 as below, which replace Fig. 2 and 3 in the original manuscript.
2. Old text in the "Material synthesis and characterization" section:

Spectra as well as fitting parameters such as the isomeric shift (IS), quadrupole splitting (QS), full width at half maximum (FWHM), evaluated percentage of the spectral component and possible assignment to the different FeF₃ structures as compared with the literature^{30,31} are presented in Fig. 2 and 3.

Correction:

Spectra as well as fitting parameters such as isomeric shift (IS), quadrupole splitting (QS), line width (LW), evaluated percentage of the spectral component from absorption (Abs.), hyperfine field (H) and possible assignment to the different FeF₃ structures as compared with the literature^{30,31} are presented in Fig. 2(a) and (b) and Table 1, respectively.

3. Old text in the "Material synthesis and characterization" section:

Mössbauer analyses confirm the formation of the major phase seen by XRD but also specify the oxidation state of iron in the amorphous phase as Fe³⁺ and can also detect other phases not crystallised enough to be seen by XRD. In the case of r-FeF₃, no other phases were detected. In the case of pyr-FeF₃, a majority of pyrochlore structure was found but some HTB-FeF₃ was also registered.

Correction:

Mössbauer analyses are used to confirm the valence of iron and to check for the presence of amorphous and insufficiently crystallised phases that cannot be seen by XRD. In the case of pyr-FeF₃, the spectrum in Fig. 2(a) confirms that the powder consists mainly of pyrochlore FeF₃ (IS = 0.47 mm s⁻¹ and QS = 0.25 mm s⁻¹, comp. 1). Four minor additional doublets are needed to complete the fitting. Among them, two components have isomer shifts corresponding to Fe³⁺ in a fluorine environment (IS > 0.40 mm s⁻¹, comp. 2 and 3) and could be assigned to either some defect in the FeF₃ or an impurity. The two other minor doublets (comp. 4 and 5) have typical hyperfine parameters corresponding to the mixed valence NH₄Fe₂Fe₆ compound. In the case of r-FeF₃, the spectrum shown in Fig. 2(b) is more complex, including paramagnetic and magnetic components with a large distribution of the hyperfine field. Only a qualitative fit could therefore be done with the data collected at room temperature. First, all spectrum components are centered around 0.4 mm s⁻¹, clearly indicating that all iron species are in the Fe³⁺ state in the sample. The paramagnetic component (comp. 1) has an isomer shift of 0.39 mm s⁻¹, suggesting that it might be in either an oxygen or a fluorine environment. The magnetic part is composed of two contributions, the first of which is a well-defined sextet (comp. 2, IS 0.48 mm s⁻¹) with typical parameters for r-FeF₃. The rest of the signal is fitted with a discrete combination of sextets (comp. 3 to 6) with virtually the same isomer shifts (~0.46–0.50 mm s⁻¹) and hyperfine fields ranging from 19 to 41 Tesla. This qualitative fitting

^a Université Clermont Auvergne, CNRS, SIGMA Clermont, Institut de Chimie de Clermont-Ferrand, F-63000 Clermont-Ferrand, France. E-mail: katia.araujo_da_silva@uca.fr

^b Université Montpellier II, Institut Charles Gerhardt de Montpellier, UMR CNRS 5253, Montpellier, France

^c Synchrotron SOLEIL, L'Orme des Merisiers Saint-Aubin, BP 48 91192 Gif-sur-Yvette Cedex, France

^d Centre National d'Etudes Spatiales, Toulouse, France



indicates a broad distribution of iron sites, probably in $[\text{FeF}_6]$ octahedra, that could be the result of different levels of amorphization, structural defects or particle sizes. Without a low temperature analysis, a more in-depth interpretation of the magnetic data is not possible.

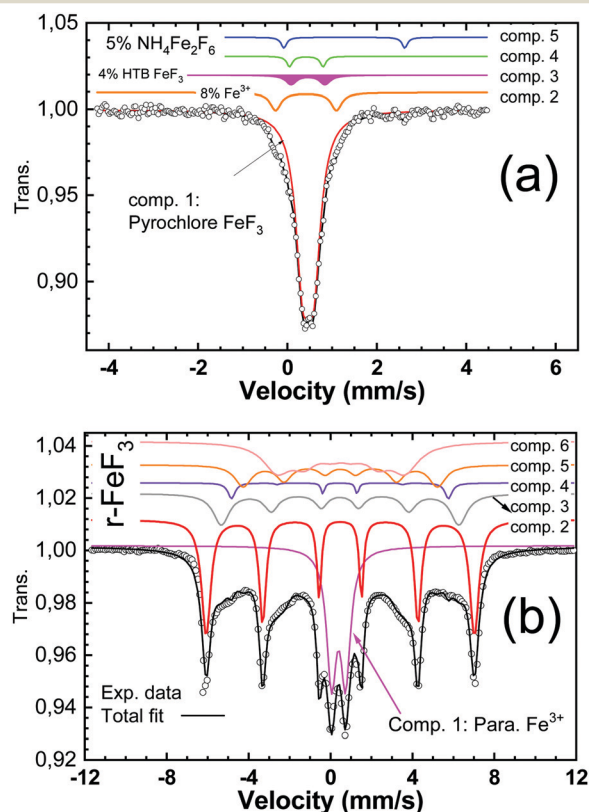


Fig. 2 ^{57}Fe room temperature Mössbauer spectra for (a) pyr- FeF_3 and (b) r- FeF_3 . The circles are the experimental data, and the black full line is the total fit. The individual components are also indicated.

Table 1 Fitted Mössbauer parameters corresponding to the spectra in Fig. 2. The error bars are typically $0.05\text{--}0.1\text{ mm s}^{-1}$ for the isomer shift, $0.1\text{--}0.2\text{ mm s}^{-1}$ for the quadrupole splitting and linewidth, $0.5\text{--}1\text{ Tesla}$ for the field and $1\text{--}2\%$ for the relative absorption areas

		IS (mm s^{-1})	QS (mm s^{-1})	LW (mm s^{-1})	Abs. (%)	H (Tesla)	Assignment
Pyro FeF_3 sample	Comp. 1	0.47	0.25	0.38	83.0	—	Pyr- FeF_3
	Comp. 2	0.42	1.36	0.29	8.0	—	Fe^{3+}
	Comp. 3	0.46	0.76	0.29	4.0	—	Fe^{3+}
	Comp. 4	0.42	0.75	0.25	2.5	—	Fe^{3+} , $\text{NH}_4\text{Fe}_2\text{F}_6$
	Comp. 5	1.27	2.71	0.25	2.5	—	Fe^{2+} , $\text{NH}_4\text{Fe}_2\text{F}_6$
		IS (mm s^{-1})	QS (mm s^{-1})	LW (mm s^{-1})	Abs. (%)	H (Tesla)	Assignment
r- FeF_3 sample	Comp. 1	0.39	—	0.55	19.1	—	Para. Fe^{3+}
	Comp. 2	0.48	—	0.25	31.8	40.6	Well defined FeF_3
	Comp. 3	0.46	—	0.66	13.5	36.0	Badly defined FeF_3
	Comp. 4	0.46	—	0.25	2.5	32.9	Badly defined FeF_3
	Comp. 5	0.48	—	0.72	10.7	29.5	Badly defined FeF_3
	Comp. 6	0.50	—	1.44	22.4	19.5	Badly defined FeF_3

The Royal Society of Chemistry apologises for these errors and any consequent inconvenience to authors and readers.

